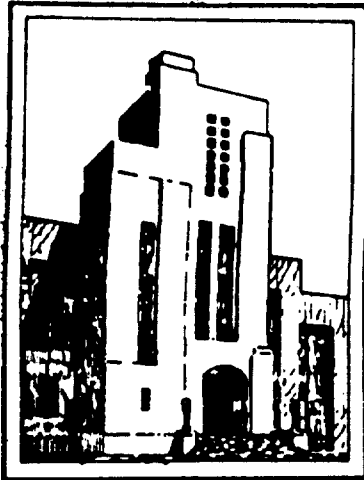


AD 628092



DEPARTMENT OF THE NAVY  
DAVID TAYLOR MODEL BASIN

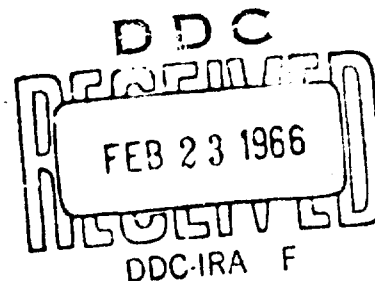
HYDROMECHANICS

TMB 3-BLADED SUPERCAVITATING PROPELLER SERIES

AERODYNAMICS

CLEARING HOUSE  
FOR  
200 05029 02  
by  
E.B. Caster  
Code 1

STRUCTURAL  
MECHANICS



APPLIED  
MATHEMATICS

HYDROMECHANICS LABORATORY  
RESEARCH AND DEVELOPMENT REPORT

August 1959

Report 1245

**TMB 3-BLADED SUPERCAVITATING PROPELLER SERIES**

**by**

**E.B. Caster**

**August 1959**

**Report 1245**

---

## TABLE OF CONTENTS

	Page
ABSTRACT .....	1
INTRODUCTION .....	1
METHOD OF APPROACH .....	1
PRESENTATION OF DATA .....	2
USE OF DIAGRAMS.....	17
CONCLUSION .....	19
ACKNOWLEDGMENT .....	19
APPENDIX – DESIGN OF A SUPERCAVITATING PROPELLER .....	20
REFERENCES .....	23

## LIST OF FIGURES

	Page
Figure 1 – $C_T - J$ Diagram for TMB 3-Bladed SC Propeller Series.....	3
Figure 2 – $C_P - J$ Diagram for TMB 3-Bladed SC Propeller Series .....	4
Figure 3 – Blade Thickness Fraction for TMB 3-Bladed SC Propeller Series .....	5
Figure 4 – Pitch Correction Coefficient ( $C_q$ ) for Finite Cavitation Numbers for TMB 3-Bladed SC Propeller Series .....	6
Figure 5 – Pitch Correction Coefficient $\Delta(P/D)$ for Finite Cavitation Numbers for TMB 3-Bladed SC Propeller Series .....	7
Figure 6 – Maximum Face Ordinate at 0.3 Radius for TMB 3-Bladed SC Propeller Series .....	8
Figure 7 – Maximum Face Ordinate at 0.5 Radius for TMB 3-Bladed SC Propeller Series .....	9
Figure 8 – Maximum Face Ordinate at 0.7 Radius for TMB 3-Bladed SC Propeller Series .....	10
Figure 9 – Maximum Face Ordinate at 0.9 Radius for TMB 3-Bladed SC Propeller Series .....	11
Figure 10 – Maximum Thickness at 0.2 Radius for TMB 3-Bladed SC Propeller Series .....	12
Figure 11 – Maximum Thickness at 0.5 Radius for TMB 3-Bladed SC Propeller Series .....	13
Figure 12 – Maximum Thickness at 0.7 Radius for TMB 3-Bladed SC Propeller Series .....	14
Figure 13 – Maximum Thickness at 0.9 Radius for TMB 3-Bladed SC Propeller Series .....	15
Figure 14 – Radial Distribution of Maximum Face Ordinates for the Propeller Design Given in the Appendix .....	22
Figure 15 – Radial Distribution of Maximum Thickness for the Propeller Design Given in the Appendix .....	22

## LIST OF TABLES

Table 1 – Coefficients for Obtaining Radial Distribution of Pitch and Blade Outline .....	16
Table 2 – Coefficients for Obtaining Face and Thickness Distribution along Chord .....	16

## NOTATION

$BTF$	Blade thickness fraction
$C_P$	Power coefficient $\left( \frac{550 P_s}{\frac{\rho}{8} \pi D^2 V_a^3} \right)$
$C_T$	Thrust coefficient $\left( \frac{T}{\frac{\rho}{8} \pi D^2 V_a^2} \right)$
$C_\sigma$	Pitch correction coefficient
$D$	Propeller diameter
$E.A.R.$	Expanded area ratio
$g$	Acceleration due to gravity
$H$	Atmospheric pressure plus the submergence pressure at 0.7 section minus the cavity pressure
$J$	Speed coefficient $\left( \frac{V_a}{nD} \right)$
$l$	Chord length
$l_{0.7}$	Chord length at 0.7 radius
$n$	Revolutions per unit time
$P_s$	Shaft horsepower
$P/D$	Pitch ratio along the radius for finite cavitation numbers
$R$	Maximum propeller radius
$R_e$	Reynolds number $\left( l_{0.7} \frac{\sqrt{V_a^2 + 0.7 \pi n D^2}}{\nu} \right)$
$r$	Radius of any propeller blade section
$S_C$	Maximum compressive stress
$T$	Thrust
$t$	Section thickness
$t_{max}$	Maximum section thickness along the radius $x$
$V_a$	Speed of advance
$(V_r)_{0.7}$	Inflow velocity to section at 0.7 radius

$x$	Nondimensional radius ( $\frac{r}{R}$ )
$x_h$	Nondimensional radius at the hub
$x_l$	Fractional distance along the chord measured from the leading edge
$y$	Pressure face ordinate
$y_{max}$	Maximum pressure face ordinate along the radius $x$
$Z$	Number of blades
$\Delta(P/D)$	Pitch correction coefficient
$\eta$	Propeller efficiency ( $\frac{C_T}{C_P}$ )
$\nu$	Kinematic viscosity
$\rho$	Density of fluid
$\sigma_{0.7}$	Cavitation number at 0.7 radius $\left[ \frac{2gH}{(V_r^2)_{0.7}} \simeq \frac{2gHJ^2}{V_a^2(J^2 + 4.84)} \right]$

## ABSTRACT

A theoretical series of 3-bladed supercavitating propellers, having a hub radius of 0.2 of the propeller radius and an expanded area ratio of 0.5, is presented. The design parameters for these propellers are plotted in the form of nondimensional coefficients which enable a complete design to be obtained.

## INTRODUCTION

Supercavitating (SC) propellers are of interest to naval architects since conventional propellers undergo a performance breakdown, because of cavitation, when operated at very high speeds. SC propellers which have fully developed cavitation on the back (suction side) of their blades, however, operate efficiently at such speeds. This report presents a theoretically derived SC propeller series and gives a method for predicting the performance of such propellers.

This series was derived theoretically rather than by the customary experimental method, since an experimental SC propeller series must be tested over a range of cavitation numbers as well as speed coefficients and this process is quite costly and time consuming. In addition, an experimental SC propeller series would not necessarily give the best propeller for a given design condition since an SC propeller, because of its section characteristics, performs satisfactorily over only a small range of speed coefficients. For these reasons the series presented here is based on theoretical calculations; however, some experimental verification of the series has been obtained.<sup>1</sup>

The main purpose of any propeller series is to provide a method for predicting the propeller performance for given design conditions and to indicate the effect of various design parameters. This derived series presents the propeller performance in the form of diagrams, including diagrams for calculating the effect of cavitation number, the propeller stress, and the offsets of the propeller blade sections. An example giving the complete design of an SC propeller is included in the Appendix.

## METHOD OF APPROACH

The series was derived by designing a number of SC propellers for operation in uniform inflow and covering a speed coefficient range from 0.3142 to 1.5708 and a nonviscous thrust coefficient range from 0.15 to 4.0. The propellers were designed for a hub radius of 0.2 of the propeller radius and an expanded area ratio of 0.5. The Reynolds numbers, used for calculating the section drag, varied from  $9.5 \times 10^6$  to  $5.7 \times 10^7$ , which corresponds to propellers having a diameter of 3 feet and operating at a speed of advance of 60 knots.

---

<sup>1</sup>References are listed on page 23.

Once these design conditions were assumed the viscous thrust and power coefficients, efficiency, and pitch ratio distribution of each design for zero cavitation number were computed. For designing a propeller and predicting its performance, two well known theories<sup>2, 3</sup> are available. One theory<sup>2</sup> deals with lightly loaded propellers in which the condition of normality is assumed and the other theory<sup>3</sup> deals with moderately loaded propellers in which the induced velocities must be calculated independently. The latter theory has been programmed for UNIVAC<sup>4</sup> and the calculations have been made for the nonviscous thrust and power coefficients, ideal efficiency, and hydrodynamic pitch distribution for zero cavitation number. Viscous corrections were applied to these calculations as described in Reference 1.

Once these propeller characteristics were obtained, calculations were extended to include finite cavitation numbers of the blade section.<sup>1</sup> These calculations resulted in a change in the pitch previously calculated for zero cavitation number, and this change is presented in the form of pitch correction coefficients. Reference 1 was also used in calculating the section shape (TMB Modified Tulin SC Section) for each design and the results of these calculations are plotted in the form of nondimensional coefficients.

## PRESENTATION OF DATA

Propeller series data can be presented as a function of various nondimensional coefficients. One set of coefficients, which enables the optimum rpm or diameter of the propeller to be easily obtained, is that of the thrust coefficient  $C_T$ , power coefficient  $C_P$ , and speed coefficient  $J$ . For this series faired curves of efficiency and pitch ratio at 0.7 radius,  $P/D_0$ , are plotted in Figure 1 as a function of  $\sqrt{C_T}$  and  $J$  and in Figure 2 as a function of  $\sqrt{C_P}$  and  $J$ . Also included in these plots are maximum efficiency lines for obtaining the optimum rpm or optimum diameter  $D$ . Because of the importance of blade stress in an SC propeller, the blade thickness fraction (*BTF*) obtained for the series is plotted next in Figure 3 as a function of  $\sqrt{C_T}$  and  $J$ .

The performance plots, Figures 1 and 2, are based on a cavitation number of zero, and since there is an effect of cavitation on the thrust and power of a propeller, this effect must be compensated for by a change in the propeller pitch. This correction to  $P/D_0$  for finite cavitation numbers of the blade section at 0.7 radius,  $\sigma_{0.7}$ , is presented in the form of two pitch correction coefficients. One of these coefficients  $C_\sigma$  is plotted in Figure 4 as a function of  $\sigma_{0.7}$  and the other coefficient  $\Delta(P/D)$  is plotted in Figure 5 as a function of  $\sqrt{C_T}$  and  $J$ . Table 1 gives the radial distribution of  $P/D$  based on the final pitch ratio at 0.7 radius,  $P/D_{0.7}$ , for operation in uniform inflow.

The section ordinates at various radii are plotted as faired curves in a series of diagrams. The maximum face ordinates  $\left(\frac{y}{l}\right)_{\max}$  at various radii are plotted in Figures 6 through 9 and the maximum thickness  $\left(\frac{t}{l}\right)_{\max}$  are plotted in Figures 10 through 13 as a function of

(Text continued on page 17.)



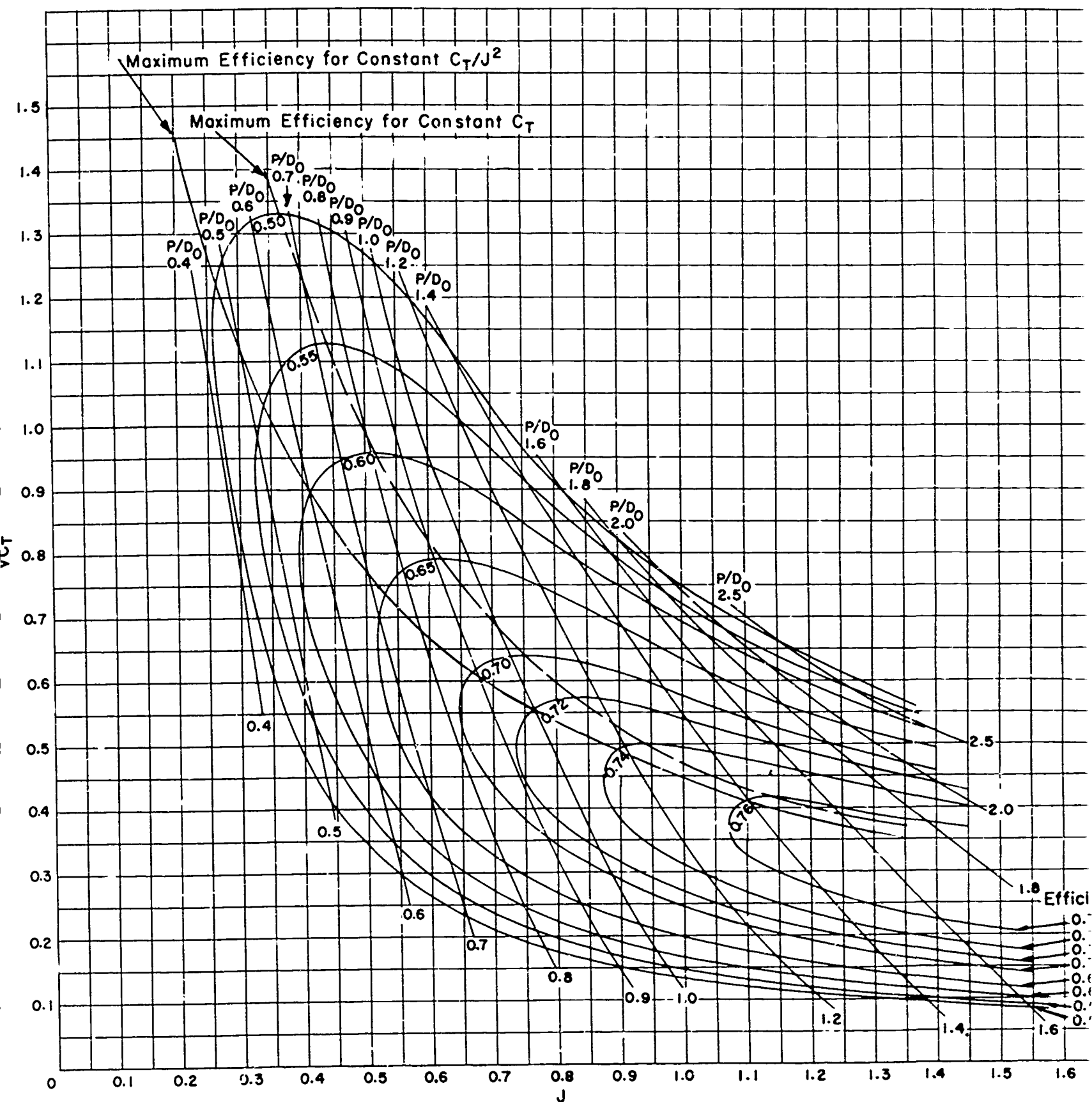


Figure 1 -  $C_T - J$  Diagram for TMB 3-Bladed SC Propeller Series

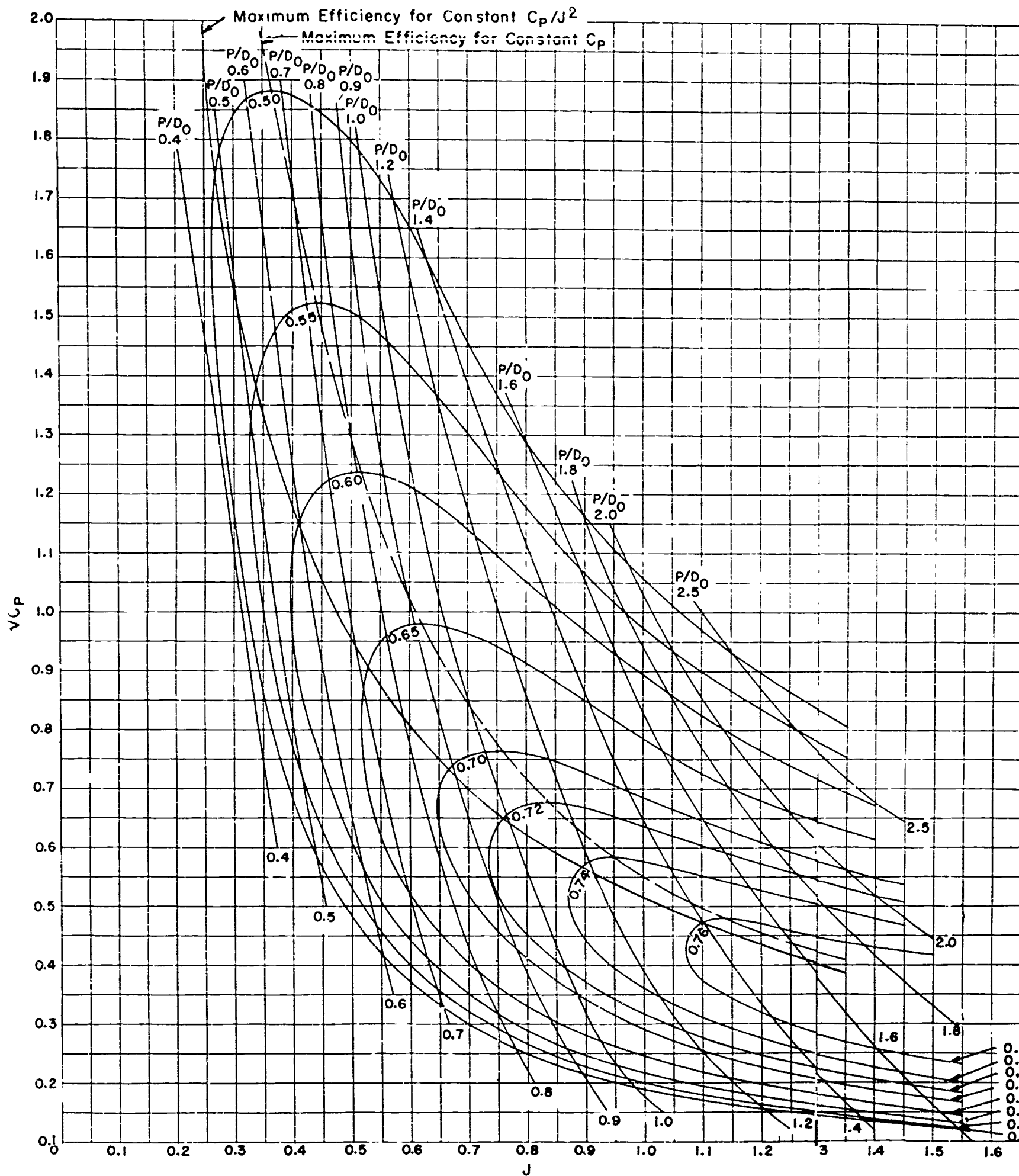


Figure 2 -  $C_p - J$  Diagram for TMB 3-Bladed SC Propeller Series

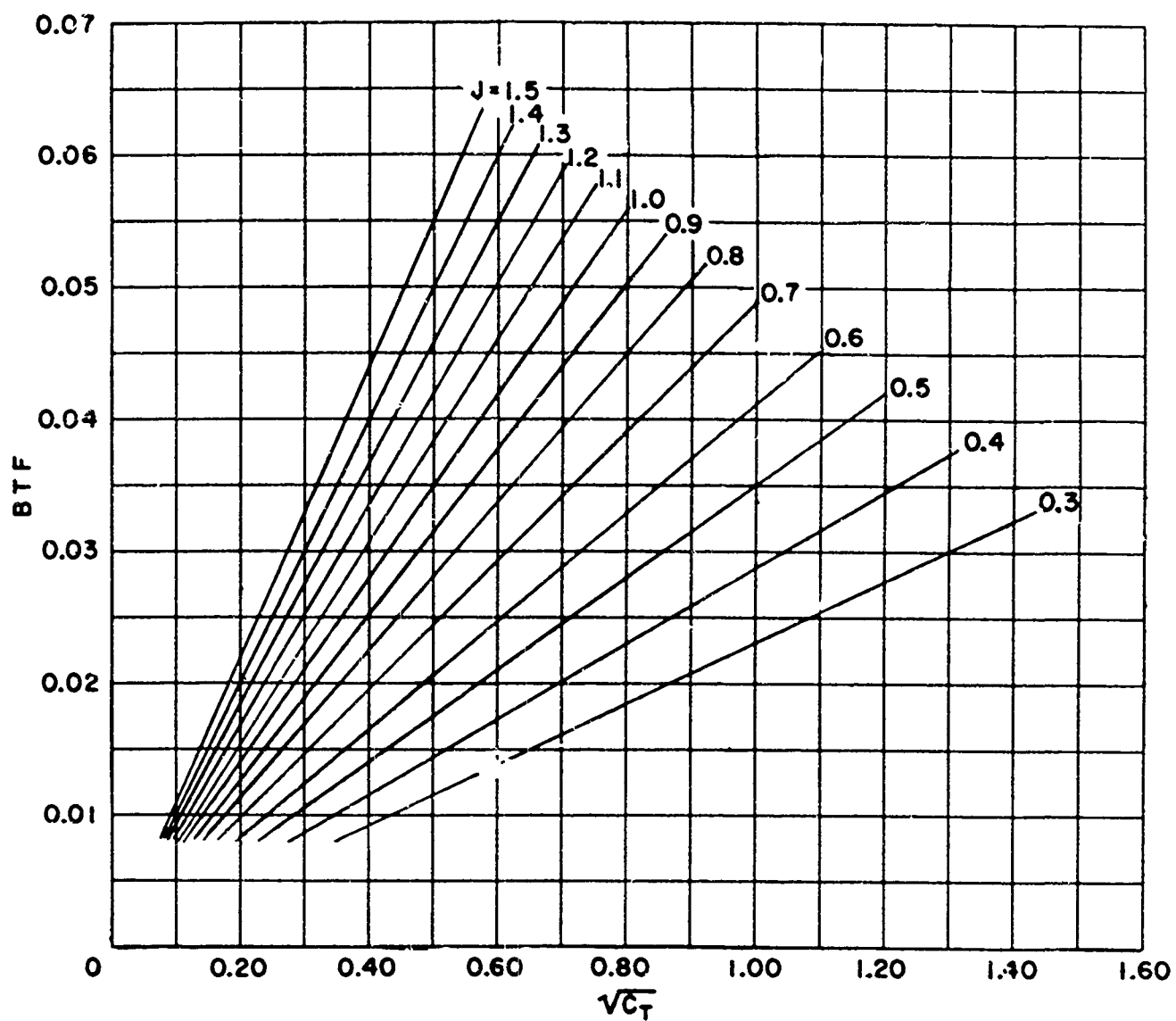


Figure 3 – Blade Thickness Fraction for TMB 3-Bladed SC Propeller Series

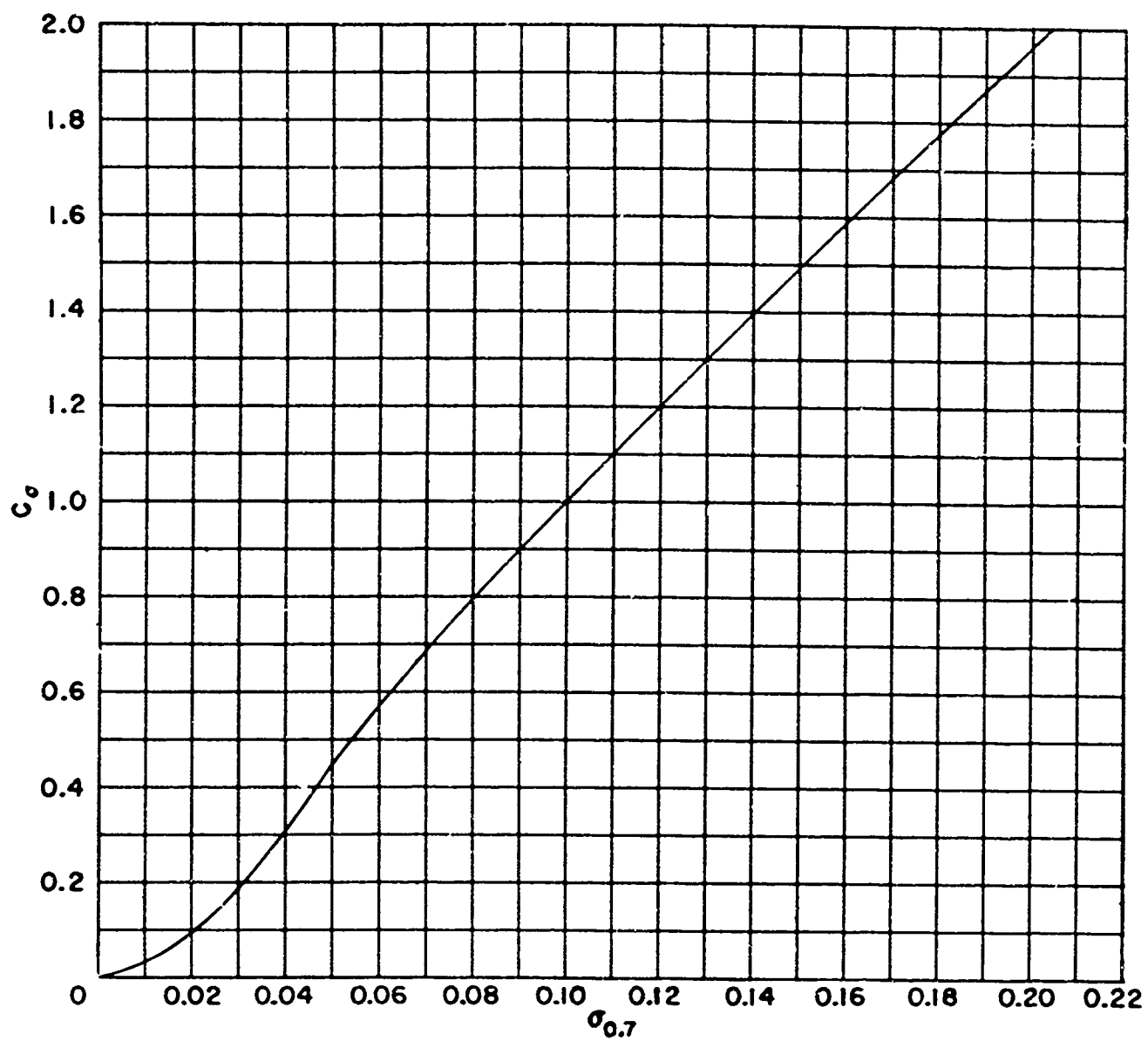


Figure 4 – Pitch Correction Coefficient ( $C_p$ ) for Finite Cavitation Numbers  
for TMB 3-Bladed SC Propeller Series

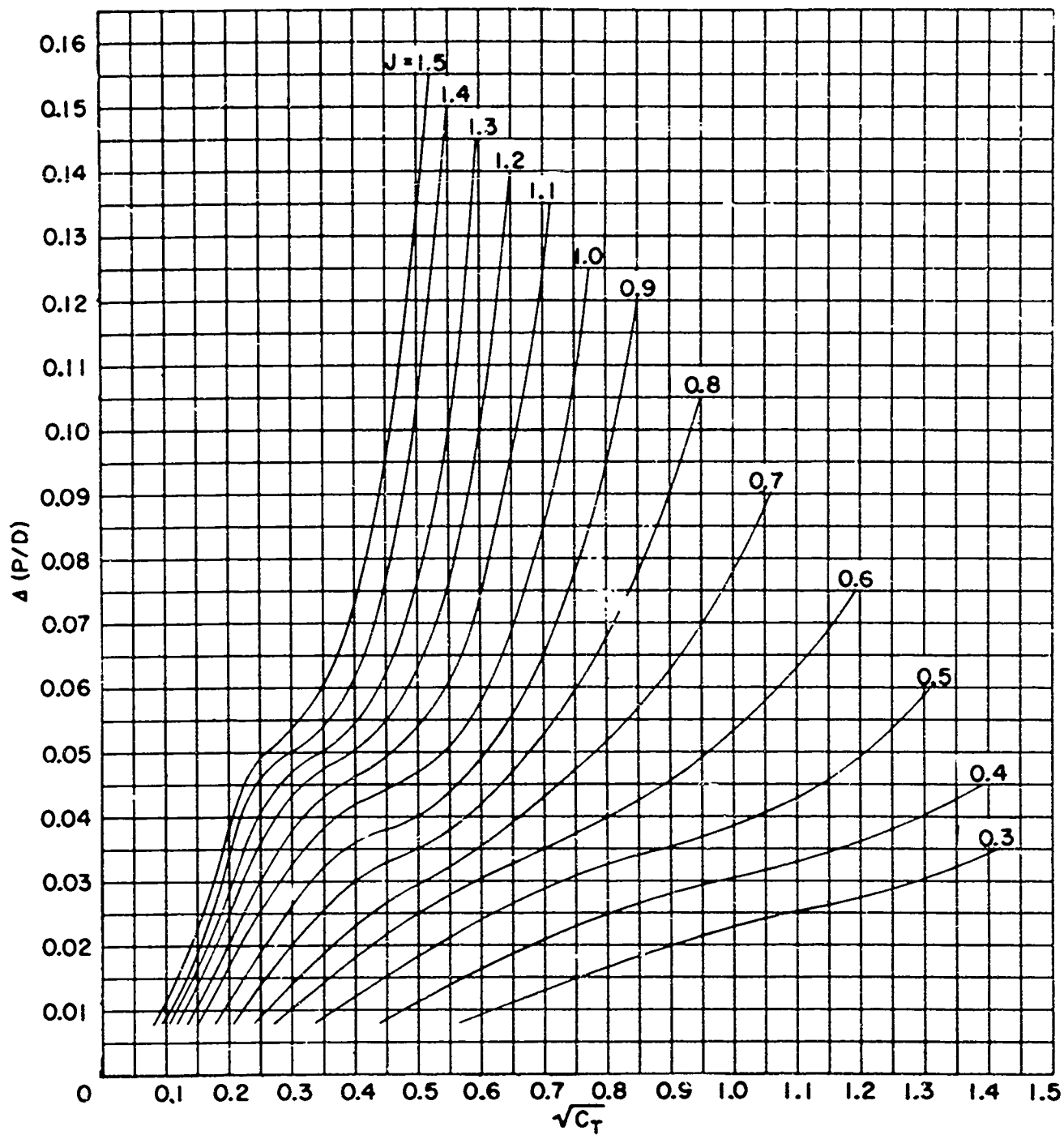


Figure 5 – Pitch Correction Coefficient  $\Delta(P/D)$  for Finite Cavitation Numbers  
for TMB 3-Bladed SC Propeller Series

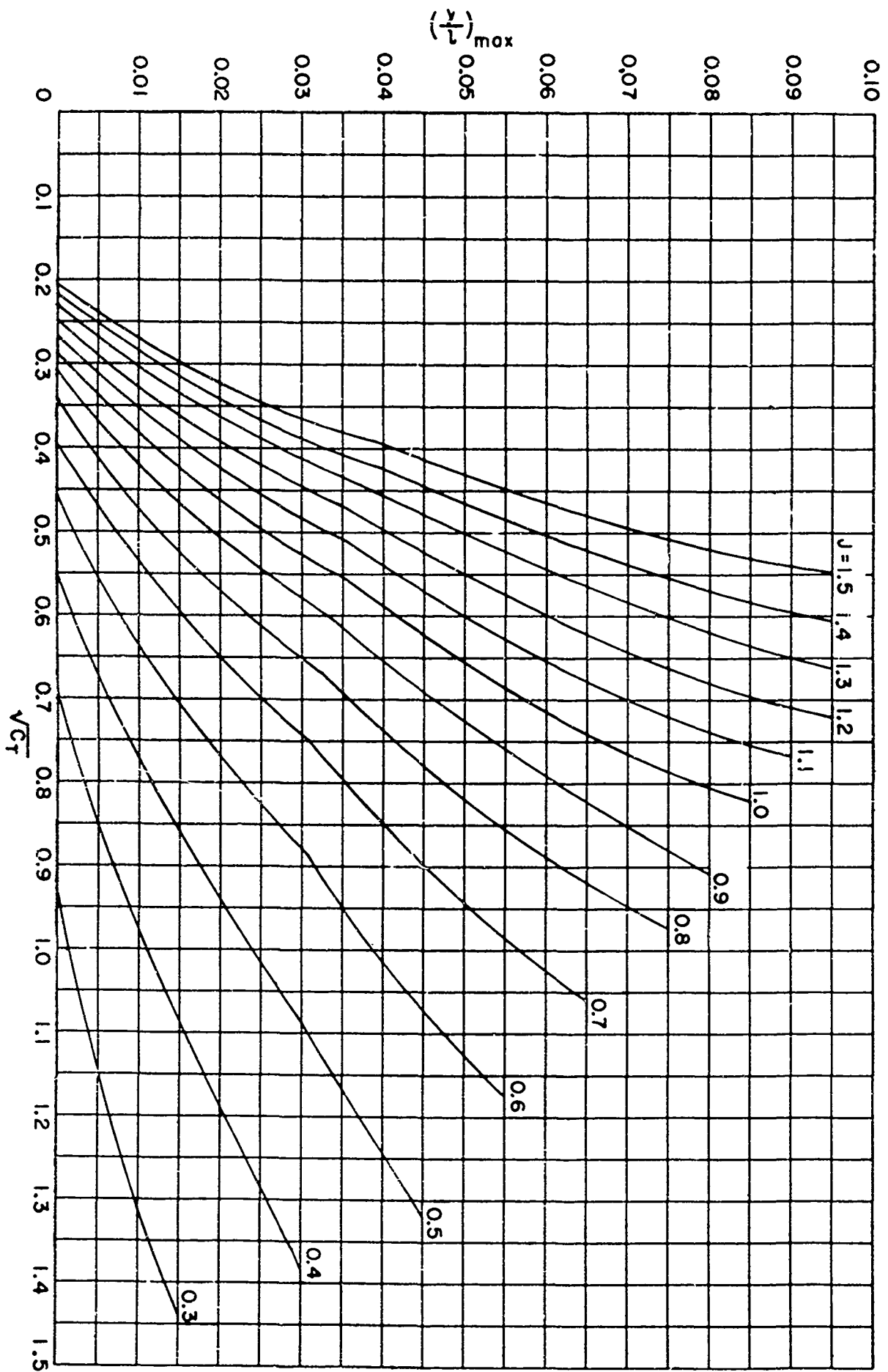


Figure 7 — Maximum Face Ordinate at 0.5 Radius for TMB 3-Bladed SC Propeller Series

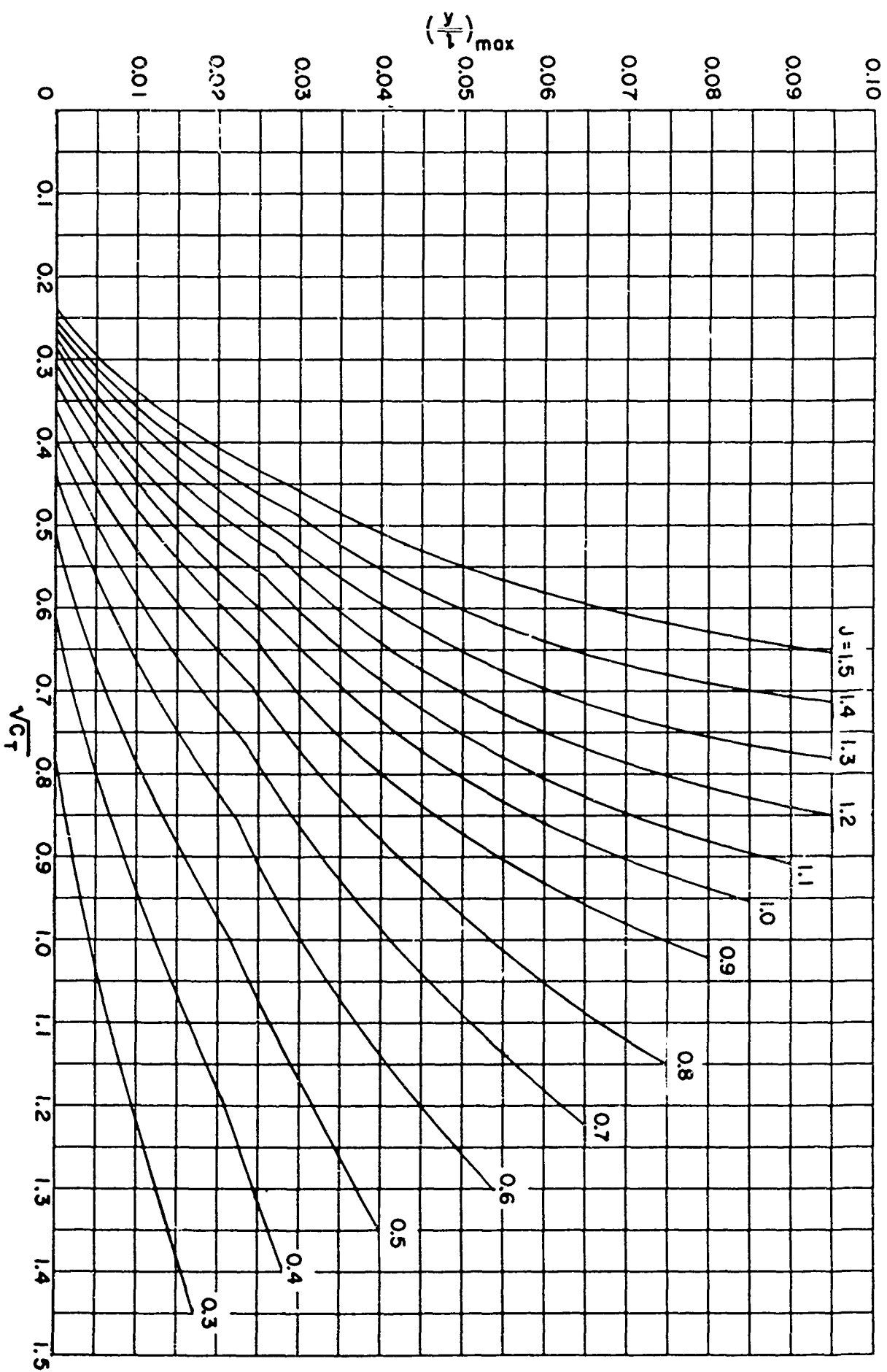


Figure 6 — Maximum Face Ordinate at 0.3 Radius for TMB 3-Bladed SC Propeller Series

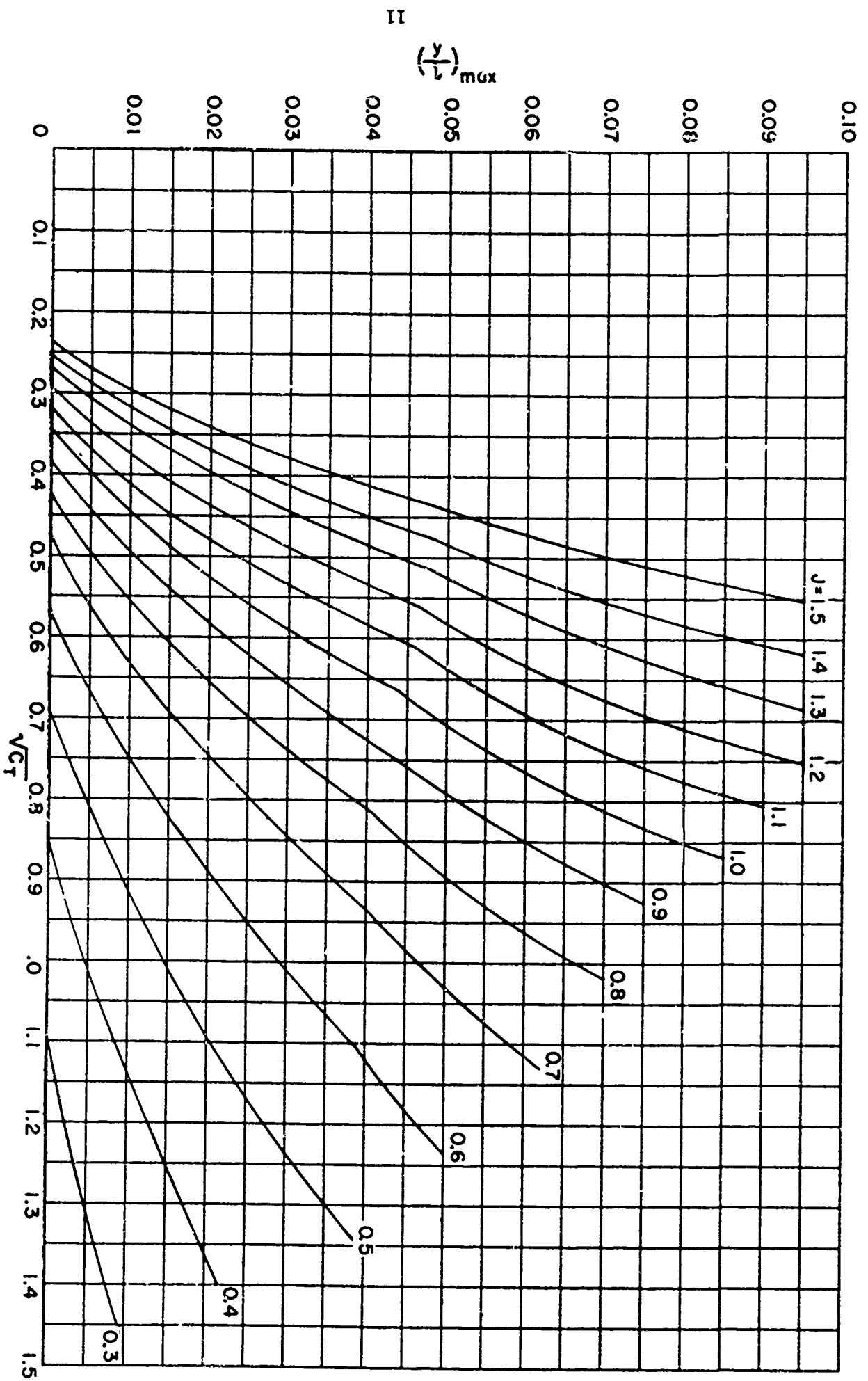


Figure 9 -- Maximum Face Ordinate at 0.9 Radius for TMB 3-Bladed SC Propeller Series



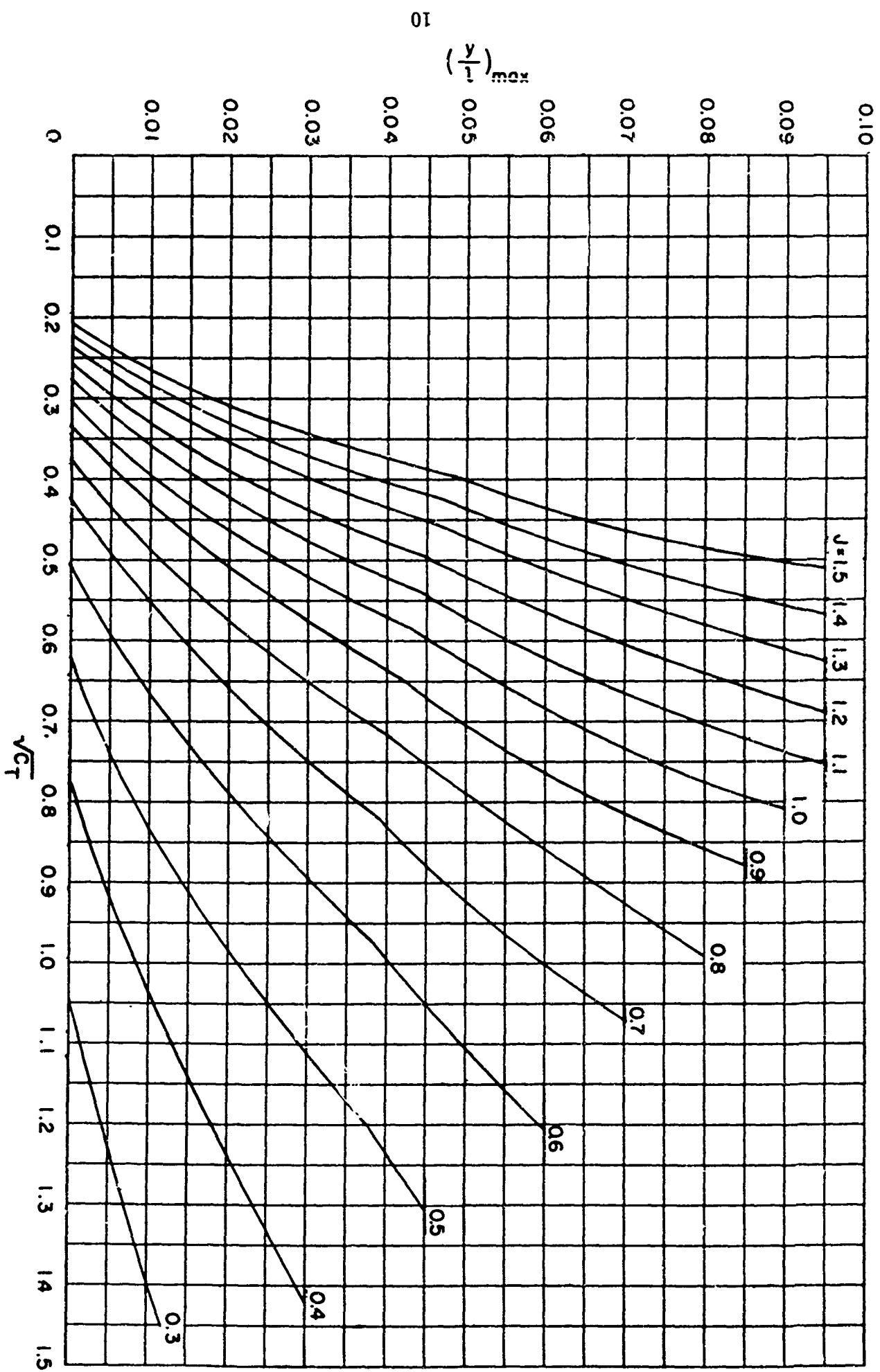


Figure 8 — Maximum Face Ordinate at 0.7 Radius for TMB 3-Bladed SC Propeller Series

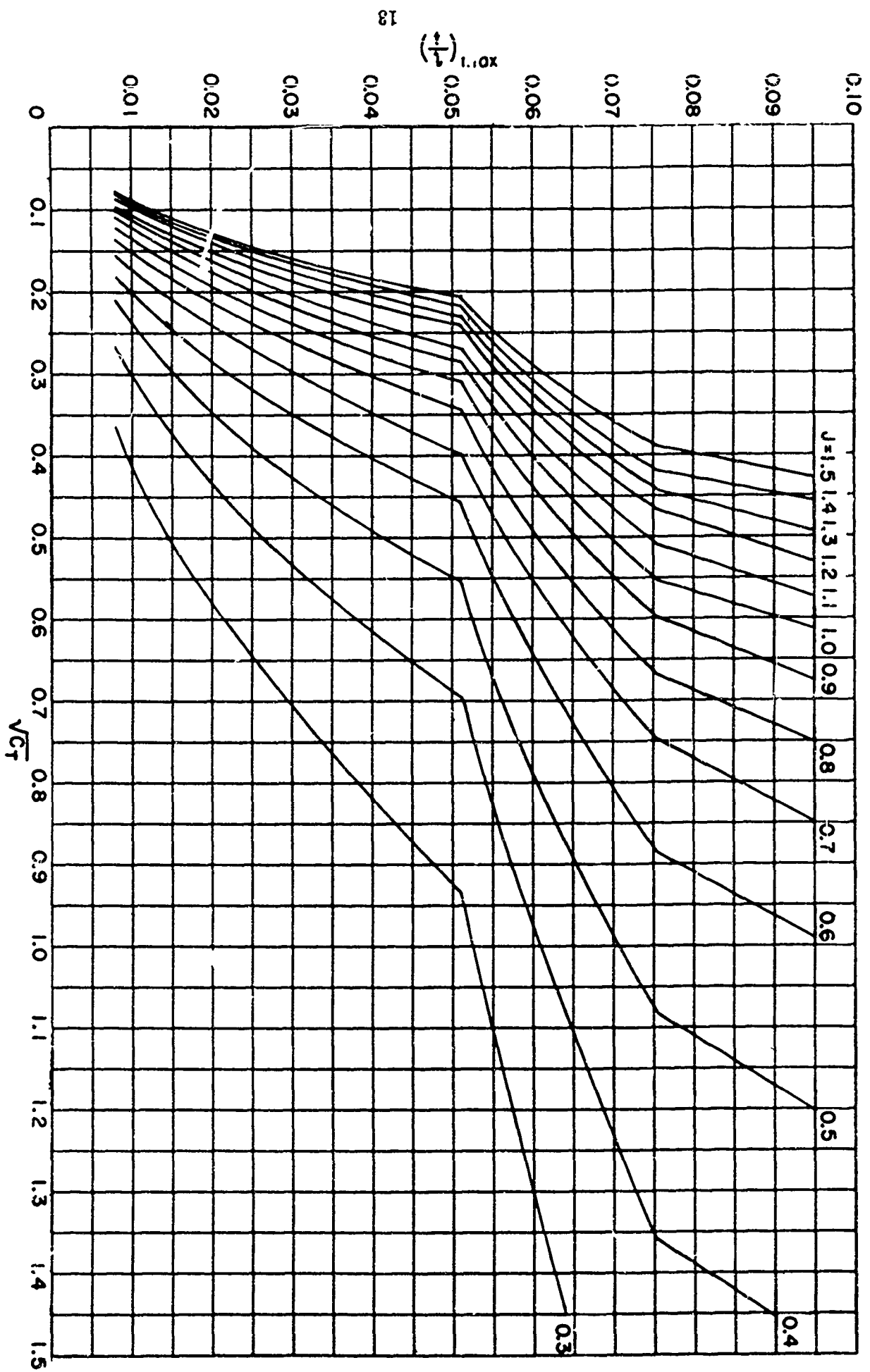


Figure 11 -- Maximum Thickness at 0.5 Radius for TMB 3-Bladed SC Propeller Series

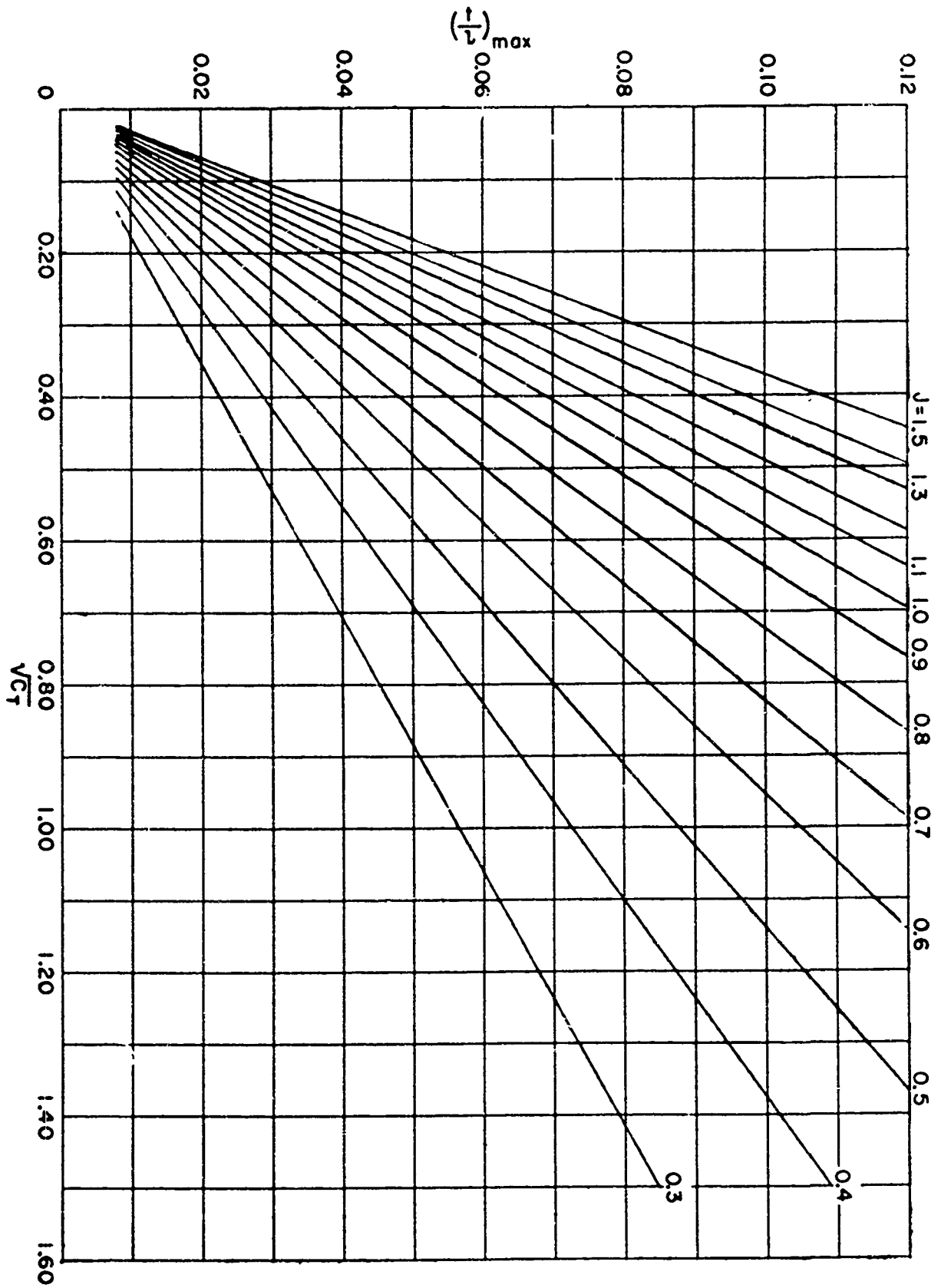


Figure 10 – Maximum Thickness at 0.2 Radius for TMB 3-Bladed SC Propeller Series

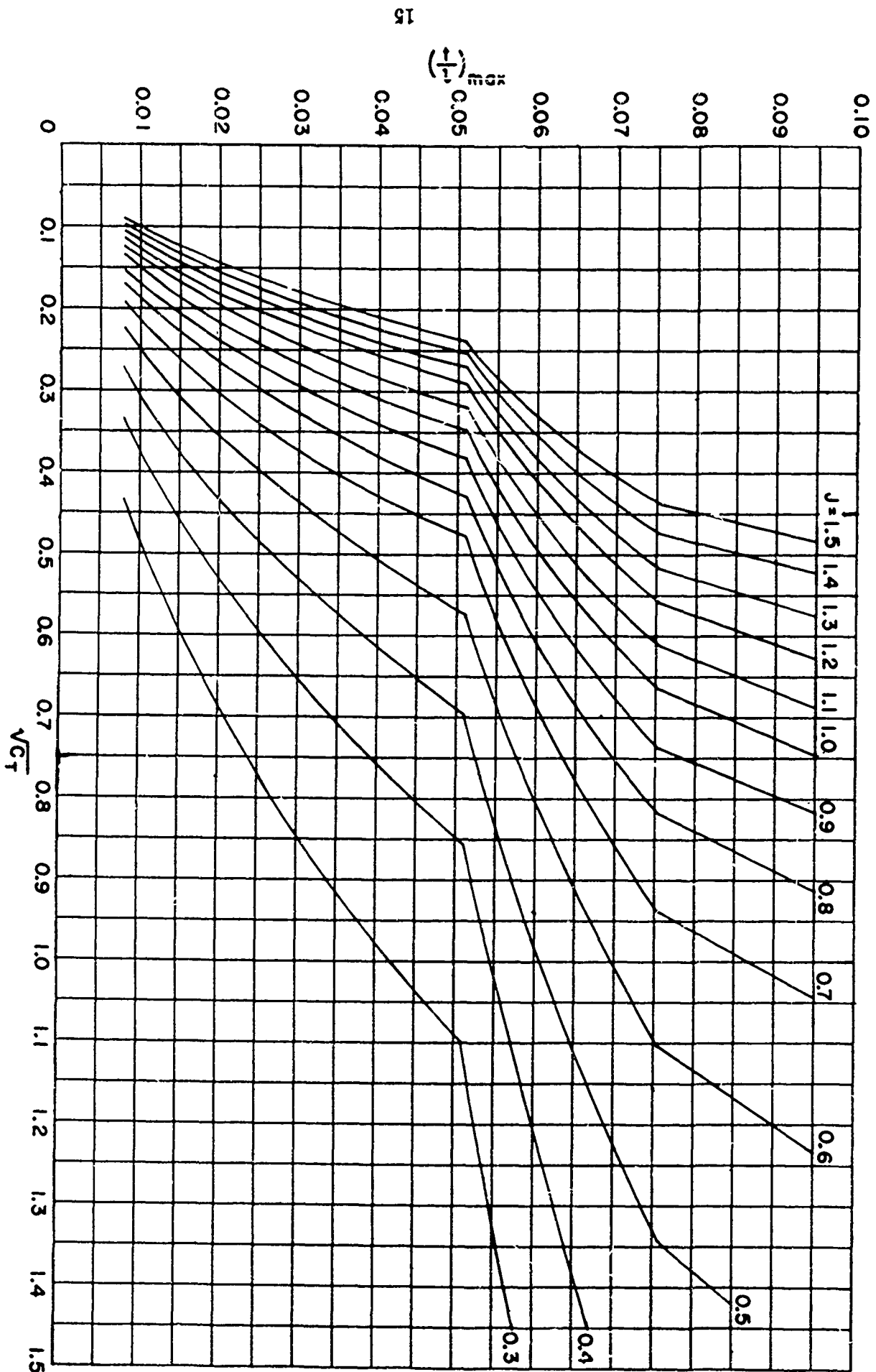


Figure 13 — Maximum Thickness at 0.9 Radius for TMB 3-Bladed SC Propeller Series

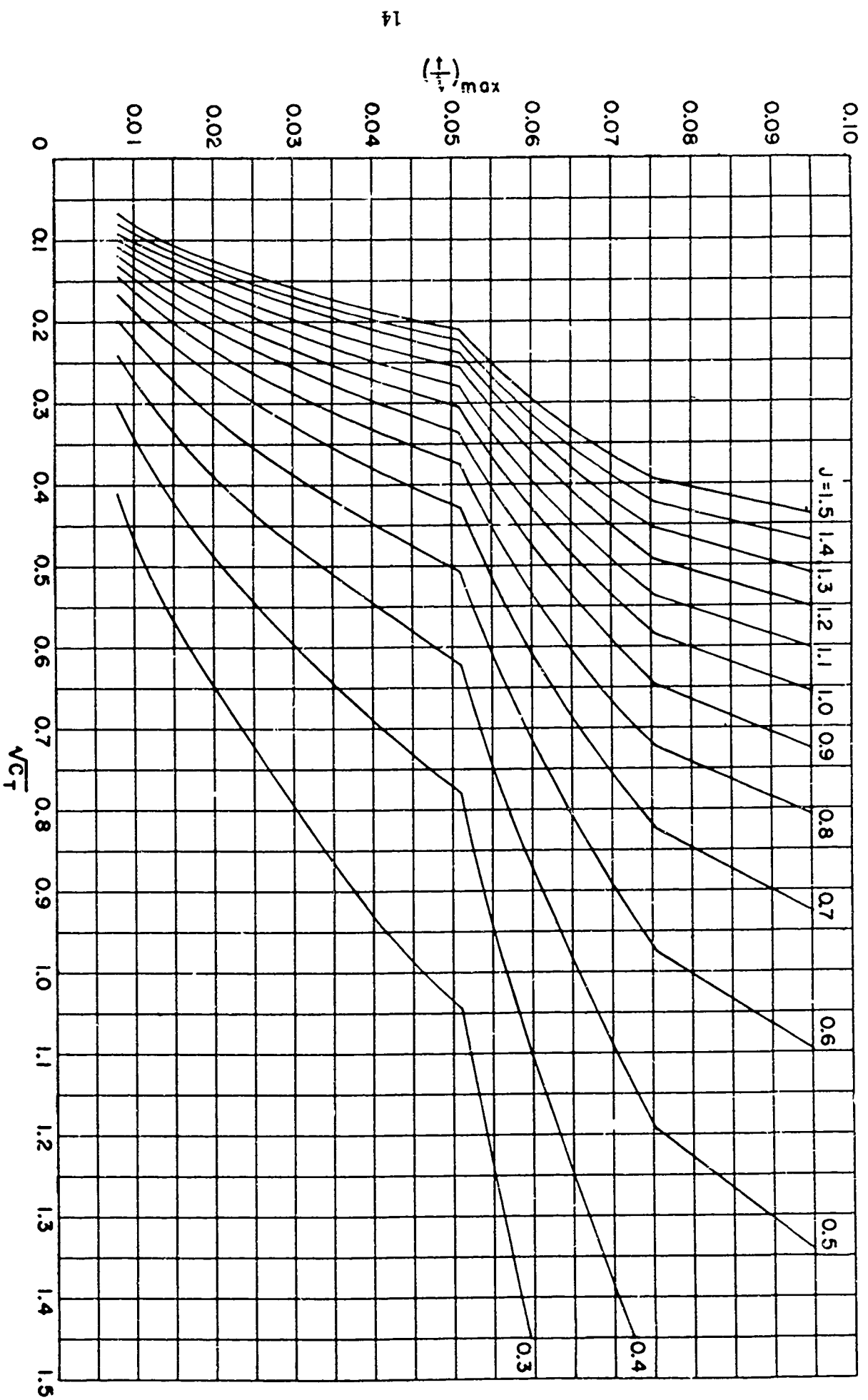


Figure 12 – Maximum Thickness at 0.7 Radius for TMD 3-Bladed SC Propeller Series

TABLE 1  
Coefficients for Obtaining Radial Distribution  
of Pitch and Blade Outline

$x$	$\frac{P/D}{(P/D)_{0.7}}$	$\frac{l}{D}$
0.2	0.974	0.382
0.3	0.979	0.382
0.4	0.984	0.382
0.5	0.990	0.381
0.6	0.995	0.373
0.7	1.000	0.351
0.8	1.006	0.306
0.9	1.011	0.230
0.95	1.011	0.167
1.0	1.010	0

TABLE 2  
Coefficients for Obtaining Face and Thickness Distribution Along Chord

$x_l$	$\frac{y}{y_{\max}}$	$\frac{t}{t_{\max}}$ when $0 < \left(\frac{t}{l}\right)_{\max} \leq 0.051$	$\frac{t}{t_{\max}}$ when $0.051 < \left(\frac{t}{l}\right)_{\max} \leq 0.0753$	$\frac{t}{t_{\max}}$ when $0.0753 < \left(\frac{t}{l}\right)_{\max}$
0	0	0	0	0
0.0075	0.0189	0.0476	0.0343	0.0297
0.0125	0.0324	0.0705	0.0501	0.0429
0.05	0.1419	0.2053	0.1326	0.1068
0.10	0.2915	0.3532	0.2124	0.1626
0.20	0.5669	0.5951	0.3421	0.2513
0.30	0.7846	0.7659	0.4453	0.3311
0.40	0.9319	0.8663	0.5285	0.4082
0.50	1.0000	0.9305	0.6075	0.4925
0.60	0.9834	0.9725	0.6879	0.5866
0.70	0.8780	1.0100	0.7787	0.6963
0.80	0.6806	1.0275	0.8645	0.8064
0.90	0.3886	1.0236	0.9401	0.9104
0.95	0.2065	1.0141	0.9719	0.9570
1.00	0	1.0	1.0	1.0

$\sqrt{C_T}$  and  $J$ . Table 1 also gives the blade outline  $l/D$  chosen for this series where  $l$  is the section chord length and Table 2 gives the chordwise distribution for the ordinates  $y$  and  $t$ . The use of these diagrams is discussed in the next section.

### USE OF DIAGRAMS

For a design based on thrust  $T$ , the propeller efficiency  $\eta$  and the pitch ratio  $P/D_0$  at 0.7 radius for zero cavitation number are obtained from Figure 1 after the nondimensional thrust coefficient  $\sqrt{C_T}$  and the speed coefficient  $J$  are calculated. Similarly, for a design based on shaft horsepower  $P_s$ , values of  $\eta$  and  $P/D_0$  can be obtained from Figure 2 once the nondimensional power coefficient  $\sqrt{C_P}$  and  $J$  are calculated. These design coefficients are obtained from the following equations:

$$C_T = \frac{T}{\frac{\rho}{8} \pi D^2 V_a^2} \quad [1]$$

$$J = \frac{V_a}{\pi D} \quad [2]$$

$$C_P = \frac{550 P_s}{\frac{\rho}{8} \pi D^2 V_a^3} \quad [3]$$

where  $\rho$  is the density of the fluid,

$D$  is the propeller diameter,

$V_a$  is the speed of advance, and

$n$  is the revolutions per unit time.

These diagrams can also be used to obtain the optimum rpm or diameter for a given thrust or power. The optimum rpm for a given diameter is obtained by plotting  $\sqrt{C_T}$  or  $\sqrt{C_P}$  on the maximum efficiency for constant  $C_T$  or  $C_P$  line in Figures 1 or 2. This point represents the  $J$  that gives the optimum rpm for a given diameter and using this  $J$ , the rpm can be calculated from Equation [2]. The optimum diameter  $D$  for a given rpm is obtained by assuming a diameter and plotting the calculated  $J$  and  $\sqrt{C_T}$  or  $\sqrt{C_P}$  on Figure 1 or 2. The  $J$  obtained at the intersection of a straight line drawn from the origin of the diagram through this point and the line of maximum efficiency for constant  $C_T/J^2$  or  $C_P/J^2$  represents the  $J$  that gives the optimum diameter for a given rpm. Using this  $J$  the optimum diameter  $D$  can be calculated from Equation [2].

If the design being considered is based on shaft horsepower, the corresponding  $C_T$  must be calculated since the remaining design diagrams are presented as a function of  $\sqrt{C_T}$  and  $J$ .

This  $C_T$  can be obtained from the efficiency  $\eta$  and  $C_P$  by the following equation:

$$C_T = \eta C_P \quad [4]$$

One of the more important aspects in the design of a supercavitating propeller is the determination of the stress since SC sections are usually thin and highly stressed. An approximate equation for calculating the maximum compressive stress  $S_C$  at the blade root, derived from Reference 5, is

$$S_C \approx \frac{0.65 \rho C_T V_a^2}{(BTF)^2} \quad [5]$$

where  $BTF$  is the blade thickness fraction from Figure 3.

As previously discussed, the final pitch is dependent upon the operating cavitation number of the propeller. The pitch correction for this effect is based on the cavitation number at 0.7 radius,  $\sigma_{0.7}$ , where

$$\sigma_{0.7} \approx \frac{2gHJ^2}{V_a^2(J^2 + 4.84)} \quad [6]$$

and where  $H$  is the atmospheric pressure plus the submergence pressure at 0.7 section minus the cavity pressure, and

$g$  is the acceleration due to gravity.

The final pitch ratio at 0.7 radius based on this cavitation number can be obtained from the equation

$$(P/D)_{0.7} = P/D_0 - \Delta(P/D)C_\sigma \quad [7]$$

where  $C_\sigma$  is the pitch correction coefficient from Figure 4, and

$\Delta(P/D)$  is the pitch correction coefficient from Figure 5.

The section shape used for an SC design is a function of the blade loading and cavity shape. Table 2 gives the chordwise distribution of the section ordinates  $y$  and  $t$  (for TMB modified Tulin SC section) once the maximum section ordinates  $y_{\max}$  and  $t_{\max}$  are obtained.

The nondimensional ordinates  $(\frac{y}{l})_{\max}$  at 0.3, 0.5, 0.7, and 0.9 radii are obtained from Figures

6 through 9 and  $(\frac{t}{l})_{\max}$  at 0.2, 0.5, 0.7, and 0.9 radii from Figures 10 through 13 for the design

$\sqrt{C_T}$  and  $J$ . Faired curves of these ordinates are drawn to obtain  $(\frac{y}{l})_{\max}$  and  $(\frac{t}{l})_{\max}$  at other radii,

where  $(\frac{y}{l})_{\max}$  from theory is zero at the hub and tip, then,  $y_{\max}$  and  $t_{\max}$  are calculated along



the radius using the chord lengths  $l$  from Table 1. An example giving the complete design of a SC propeller, using this series, is presented in the Appendix.

### CONCLUSION

A theoretically derived 3-bladed SC propeller series having a hub radius of 0.2 of the propeller radius and an expanded area ratio of 0.5 has been presented. This series provides a method for predicting the performance of an SC propeller and the effect the variation of certain design parameters have on the propeller performance.

### ACKNOWLEDGMENT

The author wishes to thank Mr. W.B. Morgan for his invaluable assistance in presenting this series.

## APPENDIX

### THE DESIGN OF A SUPERCAVITATING PROPELLER

An example for obtaining the complete design of a SC propeller is given in this section where the assumed design conditions are as follows:

$$T = 14,600 \text{ lb}$$

$$V_a = 60 \text{ knots} = 101.28 \text{ fps}$$

$$D = 3 \text{ feet}$$

$$n = 38.6 \text{ rps}$$

$$H = 36 \text{ feet}$$

$$g = 32.2 \text{ feet/sec}^2$$

$$\rho = 1.99 \text{ lb sec}^2/\text{foot}^4$$

From the above design conditions, the nondimensional design coefficients are

$$C_T = \frac{T}{\frac{\rho}{8} \pi D^2 V_a^2} = 0.202 \quad [1]$$

$$\sqrt{C_T} = 0.45$$

$$J = \frac{V_a}{nD} = 0.875 \quad [2]$$

and

$$\sigma_{0.7} = \frac{2gHJ^2}{V_a^2 (J^2 + 4.84)} = 0.031 \quad [6]$$

From Figure 1 the efficiency  $\eta$  is 4 percent and the pitch ratio  $P/D_0$  at 0.7 radius for zero cavitation number is 1.10. The maximum compressive stress  $S_C$  for this design is

$$S_C = \frac{0.65 \rho C_T V_a^2}{144(BTF)^2} = 19,400 \text{ psi} \quad [5]$$

where  $BTF = 0.031$  from Figure 3.

The final pitch ratio at 0.7 radius for this design is

$$(P/D)_{0.7} = P/D_0 - \Delta(P/D) C_\sigma = 1.03 \quad [7]$$

where  $C_\sigma = 0.2$  from Figure 4, and  $\Delta(P/D) = 0.37$  from Figure 5.

The final pitch ratio distribution  $P/D$  and radial distribution of the maximum section ordinates  $y_{\max}$  and  $t_{\max}$  are given in the following table:

(1)	(2)	(3)	(4)	(5)	(6)	(7)	(8)	(9)
$x$	$(\frac{P}{D})$	$(\frac{y}{l})_{\max}$	$(\frac{t}{l})_{\max}$	$(\frac{y}{l})_{\max}$	$(\frac{t}{l})_{\max}$	$l$ (inches)	$y_{\max}$ (inches)	$t_{\max}$ (inches)
0.2	1.00		0.0640		0.0640	13.75	0	0.880
0.3	1.01	0.0073		0.0073	0.0626	13.75	0.100	0.861
0.4	1.01			0.0106	0.0612	13.75	0.146	0.842
0.5	1.02	0.0120	0.0600	0.0120	0.0600	13.72	0.165	0.823
0.6	1.03			0.0120	0.0586	13.43	0.161	0.787
0.7	1.03	0.0110	0.0570	0.0110	0.0570	12.64	0.139	0.720
0.8	1.04			0.0085	0.0554	11.02	0.094	0.610
0.9	1.04	0.0049	0.0535	0.0049	0.0535	8.28	0.041	0.443
1.0	1.04			0	0.0515	0	0	0

Column 1 — Nondimensional radius

Column 2 — Final pitch ratio distribution  $P/D$  obtained from Table 1 where  $(P/D)_{0.7}$  is 1.03

Column 3 — Maximum face ordinates  $(\frac{y}{l})_{\max}$  at various radii obtained from Figures 6 through 9

Column 4 — Maximum thickness  $(\frac{t}{l})_{\max}$  at various radii obtained from Figures 10 through 13

Column 5 — Radial distribution of  $(\frac{y}{l})_{\max}$  obtained from a faired curve of Column 3 (Figure 14)

Column 6 — Radial distribution of  $(\frac{t}{l})_{\max}$  obtained from a faired curve of Column 4 (Figure 15)

Column 7 — Section chord length  $l$  obtained from the blade outline  $l/D$  given in Table 1

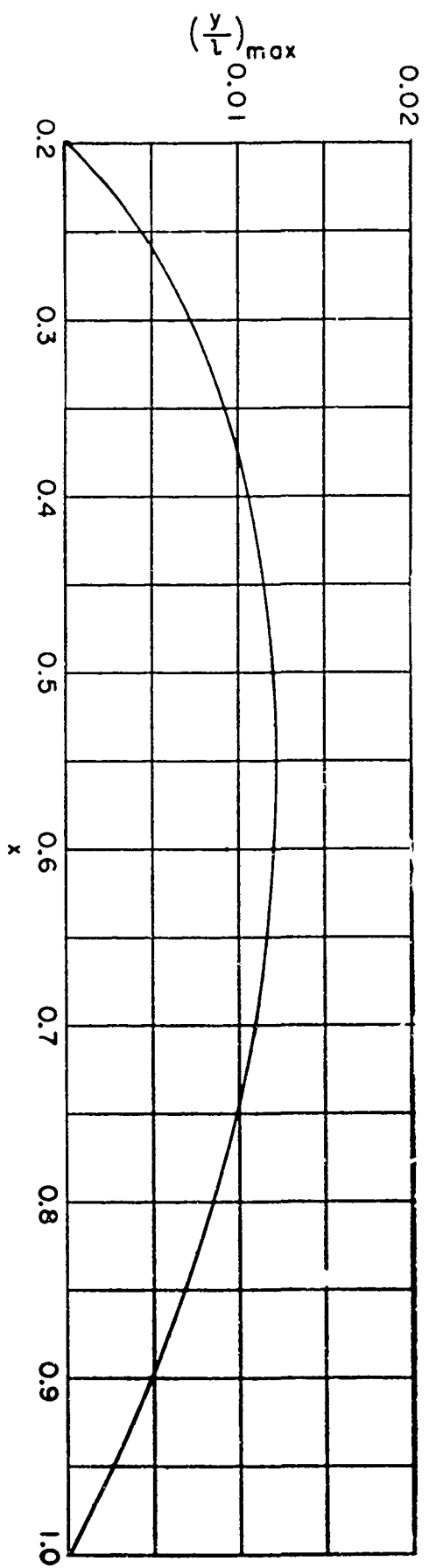


Figure 14 – Radial Distribution of Maximum Face Ordinates for the Propeller Design Given in the Appendix

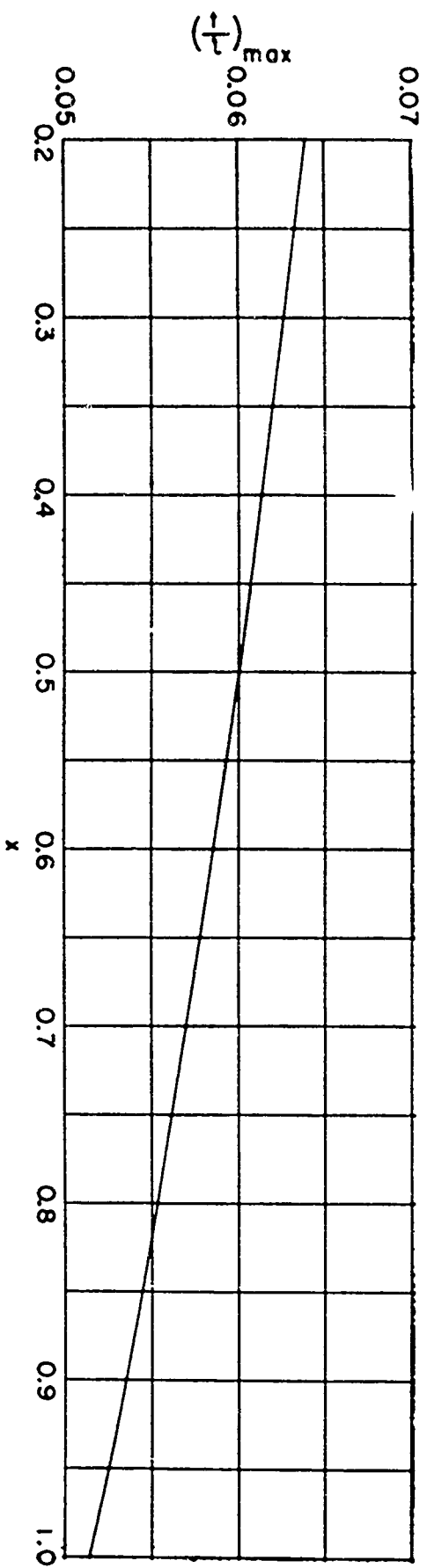


Figure 15 – Radial Distribution of Maximum Thickness for the Propeller Design Given in the Appendix

The chord distribution of the face ordinates  $y$  (pressure side) and the thickness  $t$  are given in the following table at the 0.7 radius only.

(10) $x/l$	(11) $y$ (inches)	(12) $t$ (inches)
0	0	0
0.0075	0.003	0.025
0.0125	0.005	0.036
0.05	0.020	0.095
0.10	0.041	0.153
0.20	0.079	0.246
0.30	0.109	0.321
0.40	0.130	0.381
0.50	0.139	0.437
0.60	0.137	0.495
0.70	0.122	0.561
0.80	0.095	0.622
0.90	0.054	0.677
0.95	0.029	0.700
1.00	0	0.720

Column 10 — Fractional distance along the chord measured from the leading edge

Column 11 — Chord distribution of the face ordinate ( $y$ ) at 0.7 radius obtained from Table 2, where  $y_{\max}$  is 0.139 from Column 8

Column 12 — Chord distribution of the thickness ( $t$ ) at 0.7 radius obtained from Table 2, where  $(t/l)_{\max}$  at 0.7 radius is 0.057 and  $t_{\max}$  is 0.720 from Columns 6 and 9

## REFERENCES

1. Tachmindji, A.J. and Morgan, W.B., "The Design and Estimated Performance of a Series of Supercavitating Propellers," Presented at the Second Symposium on Naval Hydrodynamics (Aug 1958).
2. Tachmindji, A.J., "Potential Problem of the Optimum Propeller with Finite Hub," David Taylor Model Basin Report 1051 (Aug 1956).
3. Lerbs, H.W., "Moderately Loaded Propellers with a Finite Number of Blades and an Arbitrary Distribution of Circulation," Transactions Society of Naval Architects and Marine Engineers (1952).
4. Hecker, R., "Manual for Preparing and Interpreting Data of Propeller Problems Which Are Programmed for the High-Speed Computers at David Taylor Model Basin," David Taylor Model Basin Report 1244 (Aug 1959).
5. Morgan, W.B., "Centroid and Moment of Inertia of a Supercavitating Section," David Taylor Model Basin Report 1193 (Aug 1957).